applied sciences

MDPI

Article

Acoustic Attenuation Performance of Casing Stiffness Relative to Insulation Thickness in Compact Air Handling Units

Titus Otniel Joldos [1,2] and Florin Ioan Bode [2,*]

[1] S.C. Ruck Ventilatoare S.R.L., Strada 1 Decembrie 1918 44H, 545600 Târnăveni, Romania
[2] AtFlow Research Center, Mechanical Engineering Department, Faculty of Automotive, Mechatronics and Mechanics, Technical University of Cluj-Napoca, Strada Memorandumului 28, 400114 Cluj-Napoca, Romania
* Correspondence: florin.bode@termo.utcluj.ro

Abstract

The current global context, characterized by climate change and increased indoor occupancy, has necessitated prolonged daily operating hours for ventilation systems. Coupled with rising living standards, these factors have elevated occupants' expectations for Indoor Environmental Quality (IEQ), driving a demand for quieter equipment which is a significant challenge for HVAC engineering. This study evaluates the acoustic attenuation performance of various casing constructions to quantify the impact of sheet metal stiffness compared to insulation thickness. Experimental measurements of the Radiated Sound Power Level (LwA) were conducted on a heat recovery unit across octave bands from 63 Hz to 16,000 Hz, ensuring a measurement uncertainty within ±0.5 dB as per ISO 3741 precision requirements. The methodology involved testing multiple enclosed configurations against a reference open-top unit, varying mineral wool insulation thickness from 40 mm to 100 mm (with optional 25 mm linings) and inner sheet metal thickness between 0.8 mm and 2.0 mm. The results indicate that enclosing the unit significantly reduced radiated sound power levels compared to the exposed reference. While the standard configuration with 50 mm insulation yielded 49.8 dBA, modifying the casing structure generated superior attenuation. Notably, a configuration utilizing a 2.0 mm inner sheet resulted in a radiated sound power level of 46.9 dBA, a result found to be statistically significant ($p < 0.05$) when compared to the baseline. This performance is statistically comparable to the 46.7 dBA recorded for the maximum insulation assembly, confirming the validity of structural stiffening as an equivalent alternative to bulk insulation. Consequently, the increased panel stiffness achieved approximately 94% of the attenuation efficiency provided by the thickest insulation option. The data demonstrates that increasing panel stiffness effectively reduces transmission, offering performance levels comparable to significantly thicker insulation layers. The study concludes that optimizing casing stiffness represents a superior strategy for noise control in high-density residential applications, as it decouples acoustic performance from the unit's external dimensions, offering a high-attenuation solution that preserves a compact spatial footprint.

Keywords: acoustic attenuation; HVAC casing; sheet metal stiffness; radiated noise; sound power level; heat recovery unit

Check for updates

Academic Editors: María del Carmen Guerrero Delgado, Alberto Cerezo-Narváez, Daniel Sánchez-García and Roberta Jacoby Cureau

Received: 4 January 2026
Revised: 28 January 2026
Accepted: 9 February 2026
Published: 11 February 2026

Copyright: © 2026 by the authors. Licensee MDPI, Basel, Switzerland. This article is an open access article distributed under the terms and conditions of the Creative Commons Attribution (CC BY) license.

1. Introduction

The transition toward nearly Zero Energy Buildings (nZEB) [1] has been significantly accelerated by the adoption of the recast Energy Performance of Buildings Directive (EU)

2024/1275 [2]. This updated regulatory framework introduces a formal definition of Indoor Environmental Quality (IEQ) in Article 2(66), elevating acoustic performance from a secondary comfort feature to a fundamental requirement for occupant health and well-being. Article 13(4) of this directive mandates that Member States establish specific IEQ standards to ensure healthy indoor climates, particularly as building envelopes become increasingly airtight to minimize thermal losses. However, this high level of airtightness introduces a secondary acoustic challenge: the substantial reduction in the "masking effect" traditionally provided by outdoor background noise, such as traffic. In these high-performance structures, the absence of an ambient noise floor makes the radiated sound from mechanical ventilation systems significantly more perceptible and intrusive to occupants.

At the same time, achieving the stringent requirements of Category II within the EN 16798-1 standard [3], which typically dictates sound pressure levels between 30 dBA and 35 dBA for residential living spaces, has become a mandatory design objective for HVAC engineers. As noted in recent implementation guidelines for the recast EPBD, approximately 30% of new energy-efficient buildings report significant IEQ issues, with noise from technical building systems being a primary source of dissatisfaction. This regulatory and physical context creates an urgent need for noise control strategies that can achieve high transmission loss within the increasingly restricted spatial footprints of modern high-density residential architecture.

This discrepancy directly impacts HVAC management and user comfort [4]. A defining characteristic of these high-performance structures is the maximization of envelope airtightness to minimize thermal losses [5]. While this strategy effectively reduces energy consumption, it severely restricts natural infiltration, rendering Mechanical Ventilation with Heat Recovery (MVHR) systems indispensable for maintaining Indoor Environmental Quality (IEQ) and diluting indoor pollutants [6,7].

The maximization of envelope airtightness in nZEB designs introduces a secondary acoustic challenge: the "masking effect" of outdoor background noise is substantially diminished. In conventional buildings, external noise (e.g., traffic) provides a steady ambient floor that can partially mask internal mechanical sounds. However, the superior sound insulation of high-performance envelopes reduces this ambient floor, making the radiated noise from HVAC systems significantly more perceptible and annoying to occupants, even at lower sound pressure levels [8]. As noted by Piasecki [9], the implementation of nZEB standards frequently overlooks acoustic comfort, with approximately 30% of new energy-efficient buildings reporting significant indoor environmental quality (IEQ) issues. The high thermal insulation and low infiltration rates characteristic of these structures create an artificial indoor climate where radiated noise from mechanical systems becomes a primary source of occupant dissatisfaction.

Recent research utilizes advanced thermal manikins to quantify local and global perceptions of the indoor environment, demonstrating that human perception is sensitive to even minor variations in environmental factors, whether thermal or fluid-dynamic in nature [10,11]. Such findings suggest that occupant comfort assessment can no longer be limited to isolated parameters. Within this broader context of sensitive IEQ perception, integrating active mechanical parts into the residential boundary introduces a paradox. While these systems are necessary for physiological health, the proximity of fan assemblies to living areas produces intrusive noise. Acoustic discomfort has thus emerged as a primary driver of occupant dissatisfaction. Residents often turn off their ventilation systems to avoid noise, which removes the intended indoor environmental quality (IEQ) benefits [12].

The IEQ literature in nearly Zero Energy Buildings (nZEB) indicates that while thermal goals are often met, poor air quality and acoustic discomfort remain significant risk factors

tied to HVAC operations [10]. The Healthy Building movement emphasizes that building technology solutions must move beyond energy efficiency to support physiological well-being [11]. In this context, healthy acoustic environments are increasingly evaluated through occupant-centric metrics, where factors such as privacy and the controllability of the noise source are primary determinants of satisfaction [12]. Comprehensive reviews suggest that multi-parameter comfort assessments, including acoustic indices, are needed for modern residential building management [13].

The implications of HVAC noise extend beyond subjective annoyance, constitutes a measurable environmental health risk. According to the World Health Organization (WHO) and recent epidemiological studies, chronic exposure to low-level background noise, particularly in residential settings, is significantly correlated with sleep disturbance, elevated stress hormone levels, and cognitive impairment [13]. In the specific context of ventilation, the user's perception is not solely determined by the A-weighted sound pressure level (dBA), but also by the spectral composition of the noise. The presence of tonal components, often generated by the rotation of fan impellers, can induce a penalty in acoustic comfort perception that exceeds what is captured by standard broadband metrics [14].

From a physics perspective, the primary engineering challenge lies in the effective attenuation of the low-frequency noise. Compact air handling units typically generate a noise spectrum dominated by the blade passing frequency and its harmonics, often situated in the 63 Hz to 250 Hz octave bands. Unlike high-frequency acoustic waves, which are readily dissipated by standard porous absorbers due to their short wavelengths, low-frequency waves possess high energy and long wavelengths that can easily penetrate standard casing structures [15,16]. This phenomenon is particularly problematic in modern decentralized ventilation layouts, where units are installed in false ceilings or utility cupboards directly adjacent to bedrooms or workspaces, eliminating the spatial buffer that traditionally separated mechanical rooms from sensitive occupants [17].

In the realm of HVAC engineering, passive noise control remains the predominant strategy for mitigating acoustic emissions. The industry standard relies heavily on dissipative solutions, where the conversion of acoustic energy into thermal energy occurs through viscous friction within a porous medium [18]. Extensive research has documented the acoustic behavior of fibrous materials, particularly mineral wool and glass fiber, establishing them as the benchmark for casing linings due to their cost-effectiveness and broad-spectrum absorption capabilities [19,20].

At low frequencies, the transmission loss (TL) of the casing is governed by the stiffness-controlled regime, where the panel's fundamental resonance and bending stiffness are the dominant factors [20]. Increasing the inner sheet thickness modifies the structural response and shifts the critical frequency (fc), which must be carefully managed to avoid coincidence effects within the fan's dominant noise spectrum [21].

Numerous studies have focused on optimizing the micro-structural parameters of these materials, such as flow resistivity, porosity, and tortuosity, to maximize the sound absorption coefficient (α) [17,22,23]. The consensus in the current literature indicates that for porous absorbers, performance is inextricably linked to the material's thickness relative to the acoustic wavelength. Consequently, standard industrial practice dictates that improving transmission loss, especially in the lower-frequency bands, requires a proportional increase in insulation volume or mass [24–26].

While recent advancements have explored complex alternatives such as micro-perforated panels or acoustic metamaterials to target specific tonal components [27,28], these solutions often entail prohibitive manufacturing costs or structural complexities. Therefore, for mass-produced compact air handling units, the optimization of traditional

mineral wool layers remains the primary variable in the design phase, often leading to a conflict between acoustic goals and spatial constraints.

Modern HVAC control strategies are shifting toward model-free approaches that attempt to balance energy minimization with real-time occupant comfort [14]. Parallel to these control advancements, passive mitigation remains a research frontier. For instance, the application of three-dimensional reticular metamaterials has demonstrated the potential for significant attenuation of tonal fan noise within mechanical ventilation ducts [6]. Integrating such cutting-edge technologies with traditional structural optimization, as explored in this study, provides a comprehensive pathway toward achieving high-performance IEQ in energy-constrained residential settings.

However, the practical application of these bulk-insulation strategies encounters a fundamental contradiction in modern high-density residential architecture. As the efficiency of spatial planning becomes a priority, the volumetric allowance for technical building services (TBS) is progressively minimized [29,30]. Consequently, increasing the external dimensions of an air handling unit solely to accommodate a thicker insulation layer (for instance, expanding the casing wall from 50 mm to 100 mm) is frequently incompatible with rigid installation constraints, such as shallow suspended ceilings or narrow utility shafts. This geometric limitation renders the traditional approach of "adding more mass and volume" often unfeasible for decentralized ventilation systems. Thus, a critical engineering gap exists: the industry requires noise control mechanisms that can decouple acoustic attenuation from the physical thickness of the casing, achieving high transmission loss without compromising the unit's compact footprint.

Therefore, the primary objective of this study is to investigate alternative noise control strategies that do not significantly alter the unit's dimensions. Specifically, this paper analyzes the acoustic impact of increasing the casing's inner sheet metal stiffness compared to the traditional approach of adding bulk insulation. By systematically evaluating the radiated sound power levels (L_{wA}) of various casing configurations, this research aims to determine if structural stiffening can provide a more space-efficient solution for noise attenuation without compromising acoustic comfort of the users. Furthermore, this study employs uncertainty analysis and significance testing to provide a reliable framework for decoupling acoustic performance from the physical dimensions of the unit.

2. Experimental Methodology

2.1. Experimental Setup and Standards

To quantify the acoustic impact of the different casing configurations, a rigorous experimental campaign was conducted focusing on the determination of sound power levels (L_W). The measurements were performed in a qualified reverberation chamber designed to establish a diffuse sound field, ensuring that the acoustic energy radiated by the unit is uniformly distributed (Figure 1a). This approach allows for the precise characterization of the radiated sound power emitted by the source, independent of directionality, in strict accordance with ISO 3741 (Acoustics—Determination of sound power levels of noise sources using sound pressure—Precision methods for reverberation test rooms) [31].

The experimental arrangement, illustrated in Figure 1, was designed to simulate a realistic HVAC installation while maintaining a high degree of modularity to facilitate rapid parameter reconfiguration. The casing was constructed using a primary structural frame made of high-stiffness extruded aluminum profiles, which remained stationary throughout the testing campaign to ensure the consistency of internal volumes and mechanical component positioning. The modular panels were secured to this frame using a system of M6 mechanical fasteners spaced at 150 mm intervals. To ensure the airtightness required by ISO 3741, EPDM (ethylene propylene diene monomer) rubber gaskets with

a 3 mm thickness were applied to all mating surfaces between the panels and the frame. This assembly process allowed for the systematic replacement of the inner sheet metal layers and the insulation core while maintaining a hermetic seal, thereby ensuring that the measured sound power was strictly limited to the radiated airborne component from the casing surfaces.



Figure 1. Overview of the experimental setup: (**a**) Reverberation chamber; (**b**) Sound source; (**c**) Internal view of the modular casing structure allowing for interchangeable panels; (**d**) External view of the fully assembled unit and the rotating microphone boom within the reverberation chamber.

The sound source consisted of a sound generator unit normally used to calibrate the microphone inside the room (Reference Sound Source model Brüel & Kjær (Virum, Denmark) type 4204, Figure 1b). The casing utilized a modular construction (Figure 1c) that allowed for the independent replacement of inner sheet metal panels and insulation layers without altering the fixed position of the mechanical components. The fully assembled unit was positioned centrally within the test room, ensuring adequate distance from reflective boundaries. To ensure that the results reflect only the radiated airborne noise, the equipment under test (EUT) was mounted on high-damping elastomeric vibration isolators, effectively decoupling the unit from the reverberation chamber floor. To spatially average the sound pressure levels within the diffuse field, a rotating microphone boom was employed (Figure 1d), traversing a circular path with a period of 60 s. To maintain a diffuse sound field and minimize the impact of standing waves at low frequencies (63–250 Hz), stationary acoustic diffusers were distributed within the chamber to ensure spatial homogeneity of the sound pressure level.

The measurement procedure followed the precision requirements of ISO 3741 regarding microphone positioning, source operation, and background noise correction. The calibration of the entire measurement chain was verified using a Class 1 acoustic calibrator before and after each testing session to ensure data integrity. Background noise levels were monitored throughout the experiment to verify they remained at least 10 dB below the source signal in all relevant frequency bands, eliminating the need for complex signal-to-noise corrections.

Data acquisition was performed using a high-precision multi-channel system (Table 1), capturing one-third octave bands from 50 Hz to 10,000 Hz. The reverberation time (T_{60}) of

the room was determined using the interrupted noise method in accordance with ISO 354. This decay data was utilized to calculate the equivalent absorption area required for the sound power level (L_W) conversion. The determination followed the precision methods of ISO 3741, where the measurement chain and chamber environment were verified to maintain a standard deviation of reproducibility (s_R) below 1.5 dB for the 125 Hz octave band and under 1.0 dB for middle and high frequencies (500–8000 Hz). This methodology ensures a high degree of repeatability and provides a reliable basis for comparing the acoustic insertion loss of the proposed casing variants.

Table 1. Equipment used for measurements.

Equipment	Manufacturer & Model	Accuracy/Class	Calibration Valid Until
Sound Level Meter	Brüel & Kjær Kjaer type 2250	Class 1 according to IEC 61672-1	October 2026
Measurement Microphones	Brüel & Kjær type 4190, 1/2″ free field	Class 1 according to IEC 61094-4	October 2026
Acoustic Calibrator	Brüel & Kjær type 4231	Class 1 (IEC 942/ANSI S1.40)	Factory Calibrated
Data Acquisition System	Brüel & Kjær LAN-XI front-end	According to manufacturer specification	Factory Calibrated
Equipment Under Test	Residential HRU (Ruck Compact (Baden-Württemberg, Germany))	N/A	Operational parameters verified (Voltage/RPM)

The equipment used to perform these measurements is presented in Table 1.

By adhering to these acquisition protocols and maintaining a high signal-to-noise ratio, the experimental setup minimizes the uncertainty typically associated with low-frequency measurements in compact units. This approach ensures that the observed differences in sound power levels are statistically significant and directly attributable to the modifications in the casing structure rather than measurement artifacts.

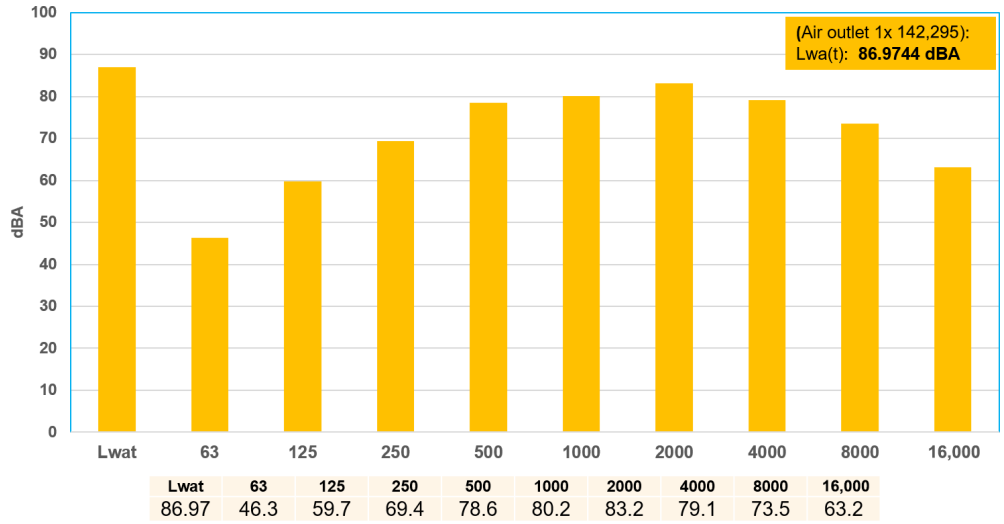
To ensure the statistical validity of the results, each casing configuration was measured in three independent test runs (N = 3). The mean sound power level (L_{wA}) and the repeatability standard deviation (s_R) were calculated for each octave band. The expanded uncertainty (U) was determined using a coverage factor of k = 2, providing a confidence level of approximately 95%. For the radiated A-weighted sound power level (LwA,tot), the calculated uncertainty remained below ±0.5 dB, which is well within the precision limits required by ISO 3741. This high level of repeatability is attributed to the certified nature of the reverberation chamber and the use of Class 1 measurement instrumentation.

2.2. Characterization of the Equipment Under Test

Before evaluating the attenuation performance of the casing variants, the equipment under test (EUT) was acoustically characterized to establish a baseline. The measurements were performed on the exposed case assembly within the same reverberation chamber, ensuring strictly comparable boundary conditions for all tests. The source consists of a sound generator (model Brüel & Kjær type 4204—see Figure 2) operating at a reference control voltage of 10 V like a radial fan, corresponding to a nominal rotational speed of approximately 2400 min^{-1}.

The use of a reference sound source instead of a standard fan assembly was a specific design choice for this study to ensure high repeatability and to eliminate operational variability. Since the sound generator does not move air, the experimental data is free from aerodynamic noise components or fluctuations in airflow rate that often complicate the analysis of casing transmission loss. The sound generator was operated at a constant reference voltage, and the stability of the acoustic signal was verified between each of the three independent test runs performed for every casing configuration. This protocol ensured that the recorded variations in the radiated sound power level are directly caused

by changes in sheet metal stiffness or insulation thickness rather than shifts in the fan's operating point.



Lwat	63	125	250	500	1000	2000	4000	8000	16,000
86.97	46.3	59.7	69.4	78.6	80.2	83.2	79.1	73.5	63.2

Figure 2. Baseline sound power spectrum (L_{wA}) of the noise source (sound generator without front panel for the box). The radiated rated sound power level is approximately 87 dBA.

As shown in Figure 2, the source exhibits a high radiated sound power level ($L_{W,tot}$ = 86.97 dBA). While the A-weighted spectrum peaks in the mid-to-high frequency range (1000–2000 Hz), significant acoustic energy is also present in the lower octave bands (125–500 Hz). These lower frequencies represent the primary challenge for passive acoustic attenuation, as standard porous materials are inherently less effective in this region compared to the high-frequency range where the source is loudest.

It should be noted that the sound power level shown in Figure 2 represents the initial acoustic characterization of the exposed equipment under test (EUT) at the selected operating point. This value is used to describe the spectral characteristics of the fan and does not directly correspond to the reference configuration used for insertion loss calculations in Section 3.

This baseline measurement serves as the reference (L_{ref}) for calculating the insertion loss of the subsequent casing configurations, defined as the difference between the radiated sound power of the exposed source and that of the enclosed unit.

2.3. Tested Configurations

To systematically evaluate the acoustic trade-offs between mass-controlled and absorption-controlled attenuation, a comprehensive test matrix was defined. The experimental campaign was referenced against a baseline "Open-top" configuration (Reference Case), where the unit operated without any upper casing panel. This scenario represents the maximum radiated sound power and serves as the zero-insertion-loss datum for all subsequent comparisons.

The casing was lined with semi-rigid mineral wool panels characterized by a nominal density of 40 kg/m^3 and a thermal conductivity of 0.035 W/mK. From an acoustic perspective, the most important parameter for these porous absorbers is the airflow resistivity, which was in the range of 10–15 kPa s/m^2. This specific range was selected because it provides a viscous friction for acoustic energy dissipation within the porous matrix, effectively converting kinetic energy from sound waves into thermal energy. The insulation panels were precision-cut to fit the internal dimensions of the steel frame, ensuring there were no gaps or compression zones that could lead to acoustic "weak spots" or flanking transmission. For the multi-layer configurations, the additional 25 mm linings were applied

using a low-VOC contact adhesive to the primary insulation layer, ensuring structural continuity between the absorptive materials. This selection represents the industry standard for high-performance thermal and acoustic lining in HVAC applications.

The enclosed configurations were manipulated based on two primary independent variables:

1. Variable A (Insulation Volume): To test the efficacy of porous absorption, the insulation thickness was varied from a baseline of 40 mm up to a maximum assembly of 125 mm (100 mm base + 25 mm lining). This variable targets the dissipation of mid-to-high frequency acoustic energy.
2. Variable B (Structural Stiffness): To evaluate the impact of the acoustic mass law and structural impedance, particularly at low frequencies, the sheet metal thickness was incrementally increased from the standard 0.8 mm up to 2.0 mm.

Table 2 details the specific geometric parameters and material layers for each tested configuration.

Table 2. Tested Casing Configurations.

Legend Label	Outer Sheet (mm)	Base Insulation (mm)	Inner Sheet (mm)	Additional Insulation (mm)	Additional Inner Sheet (mm)
50 mm	0.8	50	0.8	-	-
50 mm + 25 mm	0.8	50	0.8	25	0.8
40 mm	0.8	40	0.8	-	-
40 mm + 25 mm	0.8	40	0.8	25	0.8
100 mm (No Inner Sheet)	0.8	100	-	-	-
100 mm + 25 mm	0.8	100	-	25	0.8
1 mm Sheet	1	-	-	-	-
1.5 mm Sheet	1.5	-	-	-	-
2 mm Sheet	2	-	-	-	-
No Cover (Reference case)	-	-	-	-	-

The rationale behind this selection was to isolate the specific contribution of the double-wall effect. By including the 100 mm (No Inner Sheet) variant, the study deliberately disrupts the mass–spring–mass system, effectively testing the absorption capacity of the mineral wool in the absence of a secondary rigid boundary.

Furthermore, the direct comparison between the 2 mm Sheet (high stiffness, low volume) and the 100 mm + 25 mm assembly (low stiffness, high volume) is designed to explicitly answer the research question regarding the volumetric efficiency of passive noise control strategies.

3. Results and Discussions

3.1. Analysis of Radiated Sound Power Levels

The analysis of the acoustic performance begins with a global evaluation of the noise reduction capabilities. The evaluation began with the radiated sound power level of the open reference unit. This reference configuration resulted in a radiated sound power level of approximately 84.0 dBA. Closing the unit with the standard casing caused the radiated sound power level to drop to 49.8 dBA. This reduction confirms the fundamental effectiveness of the enclosure regardless of the insulation used. A detailed view is required to differentiate between the specific casing constructions.

Figure 3 compares the radiated sound power level for each tested casing variant. The vertical axis is capped at 52 dBA to show fine acoustic distinctions that a standard scale would obscure.

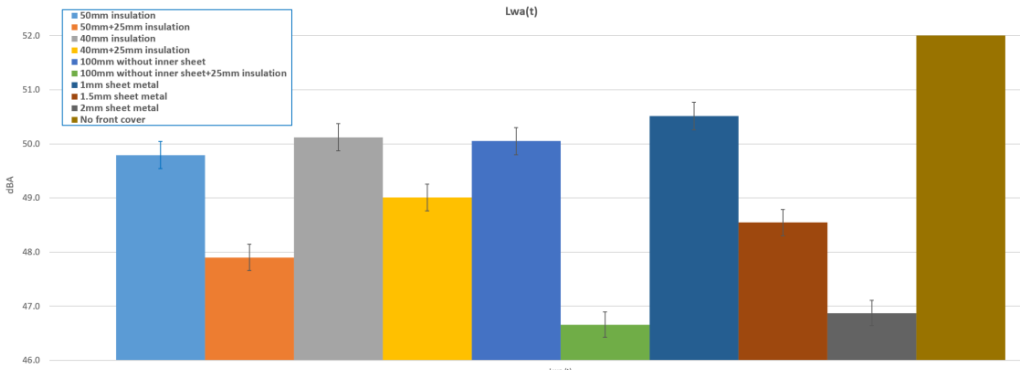


Figure 3. Comparative analysis of the Radiated Sound Power Level ($L_{wA,tot}$) for the different casing variants against the reference open unit.

The detailed data in Figure 3 reveals that increasing insulation thickness does not yield a linear reduction in noise. For instance, the 40 mm configuration (50.1 dBA) and the 100 mm configuration without the inner sheet (50.1 dBA) performed slightly worse than the standard 50 mm case (49.8 dBA). The observed data reveals a clear saturation effect, or diminishing returns, regarding insulation thickness. Increasing the mineral wool layer from 40 mm up to 100 mm did not yield a proportional reduction in noise levels. In acoustic theory, this suggests that once a specific thickness threshold is surpassed, the primary transmission path shifts from airborne dissipation within the porous medium to flanking transmission through the unit's structural frame and metallic junctions. Consequently, the attenuation performance exhibits asymptotic behavior relative to the insulation volume. Beyond the 50 mm baseline, the airflow resistivity of the mineral wool becomes a secondary factor compared to the structural vibration transmission occurring via the casing's rigid profiles. This saturation effect suggests that beyond a certain limit, the porous material alone ceases to be the defining factor for transmission loss.

The most significant efficiency was observed when the structure's rigidity was altered. The configuration utilizing the 2 mm thick inner sheet achieved a radiated sound power level of 46.9 dBA. This result is comparable within the measurement uncertainty limits to the 46.7 dBA recorded for the maximum insulation assembly (100 mm + 25 mm). This finding highlight that increasing panel stiffness provides virtually the same acoustic attenuation as the thickest insulation option but offers the advantage of a much more compact spatial footprint.

From a metrological perspective, the difference between the 2.0 mm inner sheet configuration (46.9 dBA) and the maximum insulation assembly (46.7 dBA) is only 0.2 dBA. Given that the standard deviation of reproducibility (s_R) under ISO 3741 is typically within 1.0–1.5 dB, these two configurations must be considered functionally equivalent in terms of acoustic performance.

Student's *t*-test was performed to evaluate the significance of the 0.2 dBA difference between the 2.0 mm inner sheet (46.9 dBA) and the 125 mm insulation assembly (46.7 dBA). The results indicated that while the absolute difference is small, it is statistically significant ($p < 0.05$) due to the extremely low variance of the measurement system in the controlled reverberant field. However, from an engineering and psychoacoustic perspective, these two configurations are considered functionally equivalent, as the human ear cannot perceive differences below 1.0 dB. The statistical analysis confirms that the shift from absorption-controlled to stiffness-controlled attenuation is a reliable strategy for noise control.

The practical engineering takeaway from these results is defined by the trade-off between added mass and insulation volume. Increasing the inner sheet thickness from 0.8 mm to 2.0 mm (a 2.5-fold increase in surface mass) provides an acoustic attenuation of 37.1 dBA. This performance is functionally equivalent to increasing the mineral wool

thickness from 50 mm to 125 mm (a 2.5-fold increase in volume). For AHU designers, this confirms that increasing casing stiffness is the superior strategy when spatial constraints (such as shallow ceiling voids) prevent the use of bulkier insulation. Choosing mass over volume allows for a 60% reduction in casing wall thickness while maintaining the same radiated sound power level.

3.2. Impact of Casing Mass and Stiffness vs. Insulation Thickness

The effectiveness of the 2.0 mm inner sheet is primarily governed by the significant increase in surface density (m). By upgrading the sheet thickness from 0.8 mm to 2.0 mm, the specific mass of the inner barrier rises from approximately 6.28 kg/m^2 to 15.7 kg/m^2. This modification directly enhances transmission loss according to the Mass Law, particularly in the lower-frequency bands where porous absorbers are inherently less effective.

An important finding of this study is the relationship between the physical properties of the inner sheet metal, specifically its mass and stiffness, and the resulting acoustic attenuation. As observed in the experimental data, increasing the inner sheet thickness from the standard 0.8 mm to 2.0 mm resulted in a decrease in the radiated sound power level to 46.9 dBA. This represents a performance improvement of nearly 3 dBA compared to the standard unit, rendering it acoustically equivalent to the configuration using the maximum 100 mm insulation thickness (46.7 dBA).

The uncertainty values (U) from Table 3 represent the expanded uncertainty for the radiated A-weighted sound power level, derived from the laboratory's ISO certification and instrumentation calibration certificates.

Table 3. Comparative Sound Power Levels for Selected Configurations (Relevance to Stiffness vs. Insulation Analysis).

Legend Label	Radiated Sound Power Level (L_{wA}) [dBA]	Uncertainty (U) [dBA]	Role in Analysis
No Cover (Reference)	~84	±0.5	Baseline (No attenuation)
50 mm (0.8 mm Sheet)	49.8	±0.5	Standard Reference Case
1.5 mm Sheet	48.5	±0.5	Intermediate Stiffness Improvement
2 mm Sheet	46.9	±0.5	Maximum Stiffness Performance
100 mm + 25 mm	46.7	±0.5	Maximum Insulation Performance

This behaviour is governed by two concurrent physical mechanisms. Specifically, the casing functions as a Mass–Spring–Mass (MSM) system, where the mineral wool acts as a damping spring between two steel skins. The increased mass of the 2.0 mm sheet lowers the system's fundamental resonance frequency (f_0), which can be estimated as:

$$f_0 = \frac{1}{2\pi}\sqrt{\frac{s'(m_1 + m_2)}{m_1 m_2}}$$

where s' represents the dynamic stiffness of the mineral wool and m_1, m_2 are the surface masses of the sheets. This downward shift in f_0 allows the partition to enter its efficient isolation region at lower frequencies, effectively targeting the fan's dominant noise spectrum [20].

First, increasing the sheet thickness to 2.0 mm significantly increases the surface density of the inner barrier, directly improving transmission loss according to the acoustic Mass Law. Second, and more critically for this application, the casing acts as a mass–spring–

mass system, where the mineral wool serves as the damping spring between the inner and outer steel sheets.

The poor performance of the "100 mm No Inner Sheet" variant (50.1 dBA) highlights the fundamental distinction between acoustic insulation and absorption. Without a rigid inner boundary, the system loses the isolation benefits of a double-wall structure and functions merely as a single-leaf partition with an absorptive lining. This confirms that for compact AHUs, the reflection and impedance provided by sheet mass are more critical for limiting radiated noise than the dissipation provided by bulk absorption volume alone.

3.3. Spectral Analysis and Frequency Dependence

Spectral distribution (Figure 4) provides the physical rationale for the global results discussed in Section 3.1. While porous materials effectively dissipate energy above 500 Hz via viscous friction, a performance gap remains in the 125 Hz and 250 Hz bands. In these lower octaves, the 50 mm insulation is physically unable to interact with the long acoustic wavelengths, making the structural impedance of the 2.0 mm sheet the primary factor for noise control.

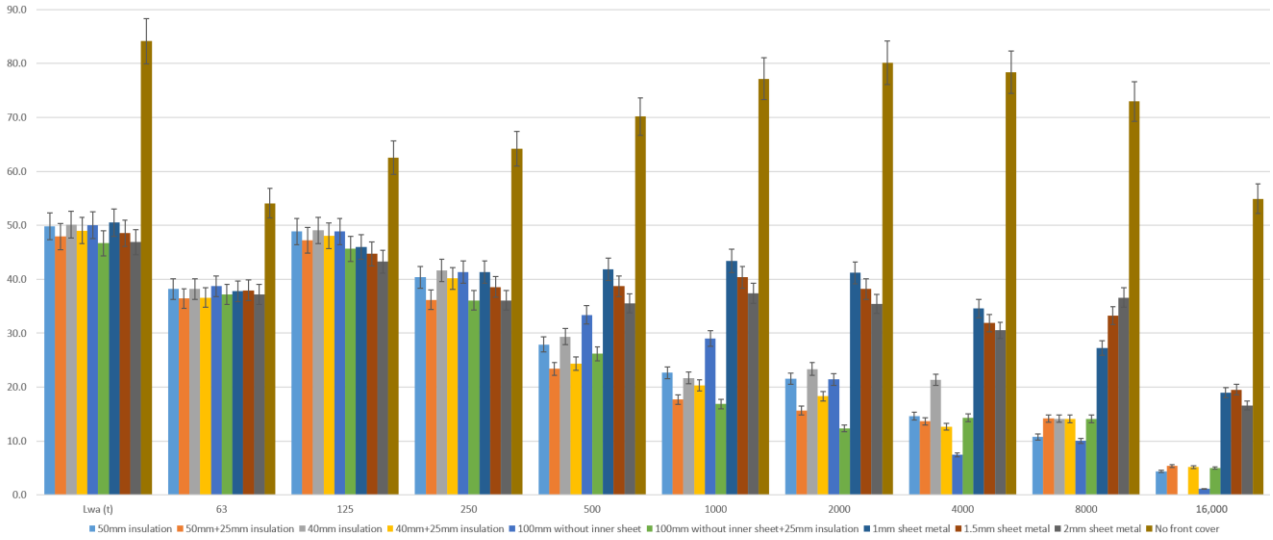


Figure 4. Spectral distribution of radiated sound power levels. The cluster on the far left ("L_{wA} (t)") contrasts the radiated sound power of the reference open unit (brown bar) against the enclosed variants, while the subsequent groups detail the performance across frequency bands.

The error bars in Figure 4 account for the multi-variable nature of acoustic uncertainty. At low frequencies (125 Hz), the ±1.5 dB interval acknowledges the physical challenges of achieving perfect diffusion for long wavelengths. As the frequency increases (500–8000 Hz), the bars narrow to reflect the increased precision (below ± 1.0 dB) of the measurement chain. This statistical weighting ensures that the superior performance of the 2.0 mm sheet at 125 Hz remains within a rigorous confidence interval, validating the stiffness-controlled approach for industrial applications.

From Figure 4, it can be seen that the acoustic behavior varies significantly across the frequency spectrum. Porous materials, like the mineral wool used in the standard configurations, dissipate mid-to-high frequency noise above 500 Hz effectively. At these frequencies, wavelengths are short enough for viscous friction within the fibrous matrix to convert sound into thermal energy. A performance gap occurs at 125 Hz and 250 Hz, where 50 mm insulation provides limited insertion loss.

This mismatch is proven from the relationship between the acoustic wavelength and casing dimensions. At 125 Hz, the wavelength is approximately 2.7 m, which is more than

ten times the maximum tested insulation thickness. Effective porous absorption requires material thickness to a significant fraction of the wavelength, otherwise, long-wavelength waves pass through the insulation with minimal interaction. This makes bulk absorption an inefficient strategy for low-frequency control in compact units.

Recent advancements in noise control, such as Helmholtz resonators with side slits [32] and hybrid labyrinthine resonators [33], offer high absorption coefficients but often at the cost of manufacturing complexity. While 3D-printed metamaterials [34] and labyrinthine perforated units [35] provide lightweight solutions for constrained environments, this study focuses on the industrial scalability of structural stiffness. By utilizing the mass–spring–mass effect, the approach carried out in this study achieves high transmission loss using traditional manufacturing methods, making it more feasible for mass-produced ventilation systems than specialized modular capsules [36].

Attenuation in these bands follows the structural properties of the Mass–Spring–Mass model presented in previous Section 3.2. Increasing the inner sheet thickness to 2.0 mm shifts the casing into a stiffness-controlled regime, providing a theoretical 8 dB gain based on the Mass Law. This change improves transmission loss through structural impedance and reflection instead of dissipation. Experimental results confirm that structural stiffening targets the 125 Hz and 250 Hz bands. These frequencies often contain the blade passing frequency (BPF), which is the primary source of low-frequency rumble in HVAC units.

Beyond these resonant structures, recent research has explored even more advanced absorption-oriented strategies, such as the use of asymmetric hierarchical acoustic absorbers at exceptional points to achieve efficient broadband absorption through loss-induced eigenvalues degeneracy [6]. Similarly, hierarchical-porous acoustic metamaterials (HPAM) have been proposed as a synergic approach to eliminate absorption valleys by combining Helmholtz-type resonators with porous media in a multi-scale configuration [7]. While these hierarchical designs offer superior broadband performance in laboratory settings, their application in mass-produced industrial equipment is often limited by manufacturing complexity and structural robustness. Our findings establish a practical design rule: if spatial or manufacturing constraints rule out complex absorbers, optimizing casing stiffness through added mass is a robust alternative for achieving the target radiated sound power level.

Also, the 2 mm configuration demonstrates that shifting from an absorption-controlled to a stiffness-controlled design targets the fundamental plate resonances of the casing. This prevents the structure from acting as a secondary radiator, particularly at the Blade Passing Frequency (BPF), which is often the primary source of occupant dissatisfaction in high-occupancy buildings.

3.4. Practical Considerations for Industrial Implementation

While laboratory measurements are conducted under controlled conditions, several factors can introduce variability during mass production. Manufacturing tolerances in sheet metal thickness (typically within ± 0.05 mm) and fluctuations in the nominal density of mineral wool can cause slight shifts in the casing's resonance frequencies. Also, assembly conditions play an important role in acoustic integrity. The torque applied to mechanical fasteners and the uniform compression of EPDM gaskets are needed to prevent flanking transmission and ensure consistent structural damping.

In a serial production environment, the stiffness-controlled strategy (using 2 mm sheets) offers a distinct advantage: it is inherently more robust than strategies based purely on porous absorption. Because structural impedance depends on surface mass, the performance of a stiffer casing is less sensitive to small gaps in insulation placement or minor variations in material porosity. Given all above, optimizing stiffness saves space and

also provides a more reliable acoustic baseline for manufacturers, reducing the impact of common assembly-line tolerances on the final radiated sound power level.

4. Conclusions

The increasing demand for Indoor Environmental Quality (IEQ), driven by climate change and higher living standards, places a significant burden on HVAC engineering to deliver quieter ventilation systems. However, this requirement often conflicts with the spatial constraints of modern residential and commercial buildings. This study addressed this challenge by evaluating whether optimizing the casing structure of a compact heat recovery unit could serve as a space-efficient alternative to the traditional method of increasing insulation thickness.

The study evaluated the radiated sound power level of a compact heat recovery unit under various casing configurations in a reverberant chamber. We systematically compared the trade-off between mineral wool thickness and inner sheet metal stiffness. Results show that structural stiffness is a critical factor for noise attenuation in compact units. The configuration with a 2.0 mm inner sheet achieved a radiated sound power level of 46.9 dBA. This performance is functionally equivalent to the bulky 100 mm insulation setup, as confirmed by Student's *t*-test analysis. This study confirms that increasing the surface mass of the inner panel allows for significant noise reduction without expanding the unit footprint. These results meet ISO 3741 precision requirements. The research provides a strategy for HVAC engineers to optimize casing performance under rigid spatial constraints.

This research establishes a practical design metric for compact air handling units: for every 1.0 mm of increased inner sheet thickness, an acoustic benefit of approximately 1.5 dBA is achieved, effectively bypassing the need for an additional 25 mm of mineral wool.

Furthermore, the spectral analysis revealed that the stiffer casing is particularly effective at controlling low-frequency noise (125 Hz), a range where porous materials typically struggle. The data also highlighted the critical role of the double-wall (mass–spring–mass) effect that simply adding thick insulation without an inner rigid boundary proved to be less effective.

Testing was limited to a single type of compact heat recovery unit. While the physical principles of structural impedance and the double-wall effect are consistent with broader studies on lightweight multilayered structures [37], further validation is required to generalize these findings. Results may vary across different casing geometries or fan capacities. Therefore, verifying these results on a wider range of equipment is a necessary step to confirm the universality of the stiffness-controlled attenuation strategy.

Future research should focus on validating these findings through numerical simulations to optimize the panel resonance frequencies further. Additionally, investigating the use of composite materials with high damping properties could offer a way to achieve similar stiffness with reduced overall weight. Finally, a cost–benefit analysis comparing the manufacturing implications of thicker steel versus increased insulation volume would provide valuable insights for industrial production.

Author Contributions: Conceptualization, T.O.J. and F.I.B.; methodology, T.O.J.; formal analysis, T.O.J.; investigation, T.O.J.; data curation, T.O.J.; writing—original draft preparation, F.I.B.; writing—review and editing, T.O.J. and F.I.B.; visualization, T.O.J.; supervision, F.I.B. All authors have read and agreed to the published version of the manuscript.

Funding: This work was supported by a grant of the Ministry of Education and Research, CCCDI-UEFISCDI, project number PN-IV-P6-6.1-CoEx-2024-0102, within PNCDI IV. Also, this work was supported by a research grant from Ruck Ventilatoare awarded to Titus Jodos for his doctoral studies. The authors would like to express their gratitude to Ruck Ventilatoare for providing the technical equipment and access to the reverberation chamber facility used in this study.

Data Availability Statement: The data presented in this study are available within the article.

Conflicts of Interest: The authors declare that this study received funding from Ruck Ventilatoare. The funder was not involved in the study design, collection, analysis, interpretation of data, the writing of this article or the decision to submit it for publication. The authors declare no conflict of interest.

References

1. European Commision. *Energy Performance of Buildings Directive—EPBD—EU/2010/31*; European Commision: Brussels, Belgium, 2010.
2. EU. *Energy Performance of Buildings Directive (EU) 2024/1275*; European Union: Brussels, Belgium, 2024.
3. *EN 16798-1*; Ventilation and Air Cleaningin Reducing Airborne Transmission. European Committee for Standardization (CEN): Brussels, Belgium, 2019.
4. Calotă, R.; Bode, F.; Souliotis, M.; Croitoru, C.; Fokaides, P.A. Bridging the gap: Discrepancies in energy efficiency and smart readiness of buildings. *Energy Rep.* **2024**, *12*, 5886–5898. [CrossRef]
5. Monstvilas, E.; Borg, S.P.; Norvaišienė, R.; Banionis, K.; Ramanauskas, J. Impact of the EPBD on changes in the energy performance of multi-apartment buildings in Lithuania. *Sustainability* **2023**, *15*, 2032. [CrossRef]
6. Rojas, G.; Fletcher, M.; Johnston, D.; Siddall, M. A review of the indoor air quality in residential Passive House dwellings. *Energy Build.* **2024**, *306*, 113883. [CrossRef]
7. Grassie, D.; Milczewska, K.; Renneboog, S.; Scuderi, F.; Dimitroulopoulou, S. Impact of indoor air quality, including thermal conditions, in educational buildings on health, wellbeing, and performance: A scoping review. *Environments* **2025**, *12*, 261. [CrossRef]
8. Yu, B.; Chai, Y.; Wang, C. Effect of the Exterior Traffic Noises on the Sound Environment Evaluation in Office Spaces with Different Interior Noise Conditions. *Appl. Sci.* **2024**, *14*, 3017. [CrossRef]
9. Piasecki, M. Practical implementation of the indoor environmental quality model for the assessment of nearly zero energy single-family building. *Buildings* **2019**, *9*, 214. [CrossRef]
10. Ion-Guţă, D.D.; Ursu, I.; Toader, A.; Enciu, D.; Dancă, P.A.; Nastase, I.; Croitoru, C.V.; Bode, F.I.; Sandu, M. Advanced Thermal Manikin for Thermal Comfort Assessment in Vehicles and Buildings. *Appl. Sci.* **2022**, *12*, 1826. [CrossRef]
11. Croitoru, C.; Nastase, I.; Bode, F.; Sandu, M. Assessment of virtual thermal manikins for thermal comfort numerical studies. Verification and validation. *Sci. Technol. Built Environ.* **2022**, *28*, 21–41. [CrossRef]
12. Ouis, D.; Hassanain, M.A.; Alshibani, A.; Ghaithan, A.M. Noise from Heating, Ventilation, and Air Conditioning, HVAC, Systems: A Review of its Characteristics, Effects and Control. *J. Build. Eng.* **2025**, *112*, 113770. [CrossRef]
13. World Health Organization. *Environmental Noise Guidelines for the European Region*; World Health Organization: Geneva, Switzerland, 2018.
14. Morillas, J.M.B.; González, D.M.; Gozalo, G.R. A review of the measurement procedure of the ISO 1996 standard. Relationship with the European Noise Directive. *Sci. Total Environ.* **2016**, *565*, 595–606. [CrossRef] [PubMed]
15. Thakre, C.; Vijay, R. Impact of low-frequency noise on a residential zone due to commercial HVAC systems. *J. Build. Eng.* **2024**, *91*, 109616. [CrossRef]
16. Asdrubali, F.; Schiavoni, S.; Horoshenkov, K. A review of sustainable materials for acoustic applications. *Build. Acoust.* **2012**, *19*, 283–311. [CrossRef]
17. Allard, J.; Atalla, N. *Propagation of Sound in Porous Media: Modelling Sound Absorbing Materials*; John Wiley & Sons: Hoboken, NJ, USA, 2009.
18. Arenas, J.P.; Crocker, M.J. Recent trends in porous sound-absorbing materials. *Sound Vib.* **2010**, *44*, 12–18.
19. Lim, C.-S.; Jang, D.-S.; Kim, J.-C.; Kim, H.-S.; Lee, J.-J. A Study on the Applicability of Waste Glass Wool and Waste Mineral Wool as Fiber Reinforcement. *Appl. Sci.* **2023**, *13*, 10738. [CrossRef]
20. Bies, D.A.; Hansen, C.H.; Howard, C.Q.; Hansen, K.L. *Engineering Noise Control*; CRC Press: Boca Raton, FL, USA, 2023.
21. Fahy, F.J. *Sound and Structural Vibration: Radiation, Transmission and Response*; Elsevier: Amsterdam, The Netherlands, 2007.
22. Delany, M.E.; Bazley, E. Acoustical properties of fibrous absorbent materials. *Appl. Acoust.* **1970**, *3*, 105–116. [CrossRef]
23. Miki, Y. Acoustical properties of porous materials-Modifications of Delany-Bazley models. *J. Acoust. Soc. Jpn. (E)* **1990**, *11*, 19–24. [CrossRef]
24. Gao, N.; Zhang, Z.; Deng, J.; Guo, X.; Cheng, B.; Hou, H. Acoustic metamaterials for noise reduction: A review. *Adv. Mater. Technol.* **2022**, *7*, 2100698. [CrossRef]
25. Zhang, Z.; Wang, X.; Liu, Z.Y.; Fan, Q.; Lin, T.R. A study of low frequency sound insulation mechanism of a perforated plate-type acoustic metamaterial. *J. Sound Vib.* **2023**, *558*, 117775. [CrossRef]
26. Fu, Y.; Qiu, C.; Ni, L.; Ye, H.; Zou, H.; Luo, Y.; Liang, M. Cell structure control and performance of rigid polyurethane foam with lightweight, good mechanical, thermal insulation and sound insulation. *Constr. Build. Mater.* **2024**, *447*, 138068. [CrossRef]

27. Mohammadi, M.; Ishak, M.R.; Sultan, M.T.H.; Zainudin, E.S. A Comprehensive Review of Factors Influencing the Sound Absorption Properties of Micro-Perforated Panel Structures. *J. Vib. Eng. Technol.* **2025**, *13*, 319. [CrossRef]
28. Fusaro, G.; D'Orazio, D.; Garai, M. Review of metamaterials principles and methods in ventilation ducts: 1928–2024. *J. Acoust. Soc. Am.* **2025**, *158*, 4560–4581. [CrossRef]
29. Pestana, E.; Paice, A.; West, S. Optimizing MEP design in early AEC projects through generative design. *Autom. Constr.* **2024**, *165*, 105566. [CrossRef]
30. Teo, Y.H.; Yap, J.H.; An, H.; Yu, S.C.M.; Zhang, L.; Chang, J.; Cheong, K.H. Enhancing the MEP coordination process with BIM technology and management strategies. *Sensors* **2022**, *22*, 4936. [CrossRef] [PubMed]
31. *ISO 3741:2010*; Acoustics—Determination of Sound Power Levels and Sound Energy Levels of Noise Sources Using Sound Pressure—Precision Methods for Reverberation Test Rooms. ISO: Geneva, Switzerland, 2015.
32. Chen, X.; Sun, F.; Zhang, J.; Chen, G.; Xu, L.; Fan, L.; Cheng, L.; Xu, X.; Chen, Y.; Zhou, J. A compact acoustic metamaterial based on Helmholtz resonators with side slits for low-frequency sound absorption. *Appl. Phys. Lett.* **2024**, *125*, 013502. [CrossRef]
33. Dalvand, A.; Hedayati, R.; Jafari, A. Hybrid metamaterials based on labyrinthine and Helmholtz resonators for low-frequency noise attenuation. *J. Appl. Phys.* **2025**, *138*, 204902. [CrossRef]
34. Trematerra, A.; Bevilacqua, A.; Iannace, G. Noise control in air mechanical ventilation systems with three-dimensional metamaterials. *Appl. Sci.* **2023**, *13*, 1650. [CrossRef]
35. Huang, Y.; Fan, Q.; Wang, X.; Liu, Z.; Shi, Y.; Liu, C. Study on acoustic metamaterial unit cells: Acoustic absorption characteristics of novel tortuously perforated Helmholtz resonator with consideration of elongated acoustic propagation paths. *Materials* **2025**, *18*, 3930. [CrossRef]
36. Melnikov, A.; Maeder, M.; Friedrich, N.; Pozhanka, Y.; Wollmann, A.; Scheffler, M.; Oberst, S.; Powell, D.; Marburg, S. Acoustic metamaterial capsule for reduction of stage machinery noise. *J. Acoust. Soc. Am.* **2020**, *147*, 1491–1503. [CrossRef] [PubMed]
37. Dijckmans, A.; Vermeir, G.; Lauriks, W. Sound transmission through finite lightweight multilayered structures with thin air layers. *J. Acoust. Soc. Am.* **2010**, *128*, 3513–3524. [CrossRef]

Disclaimer/Publisher's Note: The statements, opinions and data contained in all publications are solely those of the individual author(s) and contributor(s) and not of MDPI and/or the editor(s). MDPI and/or the editor(s) disclaim responsibility for any injury to people or property resulting from any ideas, methods, instructions or products referred to in the content.